A Low Cost Counter Electrode Using Poly(Brilliant Cresyl Blue) and Multi-Walled Carbon Nanotubes For Dye-Sensitized Solar Cells

Kuo-Chiang Lin, Jia-Yan Huang, Shen-Ming Chen[*]

Electroanalysis and Bioelectrochemistry Lab, Department of Chemical Engineering and Biotechnology, National Taipei University of Technology, No.1, Section 3, Chung-Hsiao East Road, Taipei 106, Taiwan (ROC).
[*]E-mail: smchen78@ms15.hinet.net

An inexpensive poly(brilliant cresyl blue) (PBCB) is used as a substitute for platinum to construct the counter electrode in dye-sensitized solar cells (DSSCs). The PBCB counter electrode with multi-walled carbon nanotubes (MWCNT) approaches lower charge-transfer resistance and higher electrocatalytic activity for the I_3^-/I^- redox reaction by controlling the PBCB formation on MWCNT in the preparation procedure with more scan segments. The overall energy conversion efficiency of the DSSC is reaching more higher with more scan segments prepared PBCB counter electrode. Particularly, both the PBCB deposition amount and the efficiency are enhanced by MWCNT. This photoelectric properties, simple preparation procedure and inexpensive cost allow MWCNT-PBCB electrode to be a low cost counter electrode for DSSCs.

1. INTRODUCTION

Dye-sensitized solar cells (DSSC) have currently attracted widespread academic and commercial interests for the conversion of sunlight into electricity because of their low cost and high efficiency since reported by O'Regan and Grätzel [1–3]. In order to further improve the performance of DSSC, extensive research has been conducted on each constituent of the solar cells such as semiconductor nano-crystalline [4], dye molecules [5], electrolytes [6], and counter electrodes [7].

Counter electrode (CE) is a critical component of DSSC, which serves as a mediator for collecting electrons from external circuit and reducing I_3^- ions to I^- ions so as to regenerate the redox

couple. Platinized counter electrode has been widely used in DSSC so far, due to its high conductivity and catalytic activity for reduction of I_3^- ions. However, platinized CE is restricted by high cost and corrosion of platinum in the presence of I^-/I_3^- redox in electrolyte [7], it is desirable to develop low-cost and more stable materials such as carbon-based materials [8 − 13] (carbon black, graphite, mesoporous carbon, carbon nanotubes) and conducting polymers including poly(3,4-ethylenedioxythiophene) [14,15] and polyaniline (PANI) [16,17] as more economic alternatives to platinized CE. As a well known conducting polymer, polypyrrole (PPy) has attracted more and more research interests as a potential candidate for platinized counter electrode because of its facile synthesis, high catalytic activity and considerable environmental stability [18,19].

Chemically prepared PANI CE mentioned above required complicated fabrication processes, moreover, the instability of catalytic activity and adhesion to glass substrate were also inevitable. On the other hand, electropolymerization method has been successfully employed to prepare polythiophene derivative polymer film as CE of DSSC [14,20], and homogeneous and well adhesive polymer film could be obtained on ITO (indium tin oxide) glass.

Carbon [21] and conducting polymer [22] were also proposed to be the catalyst for I_3^- reaction in DSSCs, but these new materials are still in early stage of development. Because of its low catalytic activity compared with platinum, it requires a thick porous film to obtain an acceptable catalytic effect, and the mechanical stability is still in concerned. Recently, PVP-capped Pt nanoclusters deposited on TCO glass as the counter electrode for DSSCs was developed by Wei et al. [23,24]. It showed the good catalytic performance and ultralow Pt loading by using this cheap wet process to manufacture the DSSC counter electrode. Carbon nanotubes (CNT) have been extensively used in electrode modification for electrochemical studies [25-37].

In azine dyes brilliant cresyl blue (BCB) is a cationic quinine-imide dye with a planar rigid structure with promising properties as a redox catalyst with features like fast rate of charge transfer and ion transport [38–40]. The poly(brilliant cresyl blue) (PBCB), with good electrocatalytic properties, can be easily synthesized by electrochemical polymerization of BCB. It has potential to be used as a counter electrode material for DSSCs.

In this work, we plan a low cost counter electrode using an inexpensive BCB material electropolymerized on MWCNT to enhance the activity for I_3^- reaction. The use of MWCNT and the PBCB deposition amount are the main parameters to investigate regarding to the electrochemical and spectrometric characteristics and the cell efficiency.

2. MATERIALS AND METHODS

2.1. Reagents

Brilliant cresyl blue (BCB), multi-walled carbon nanotubes (MWCNT), P25 TiO_2 powder, N719 dye, 4-t-butylpyridine (TBP), Triton X-100 solution and PEG 20000 were purchased from Sigma-Aldrich (USA). Indium tin oxide (ITO) ($7\Omega \cdot cm^{-2}$) was purchased from Merck Display Technologies (MDT) Ltd (Taiwan). Lithium iodide (LiI, analytical grade), potassium iodide and iodine

(I_2, analytical grade) were obtained from Wako (Japan). 60 μm thick surlyn films were purchased from Solaronix S.A., Aubonne, (Switzerland). All other chemicals (Merck) used were of analytical grade (99%). Double distilled deionized water was used to prepare all the solutions.

2.2. Apparatus

All electrochemical experiments were performed using CHI 1205a potentiostats (CH Instruments, USA). The working electrode was glassy carbon electrode (GCE) using BAS GCE (with diameter of 0.3 cm, geometric surface area of 0.07 cm^2, Bioanalytical Systems, Inc., USA). Electrochemical experiments carried out with a conventional three-electrode system which consisted of an Ag/AgCl (3 M KCl) as a reference electrode, a GCE as a working electrode, and a platinum wire as a counter electrode. The buffer solution was entirely altered by deaerating with nitrogen gas atmosphere. The electrochemical cells were kept properly sealed to avoid the oxygen interference from the atmosphere. Prior to modification, the GCE was mechanically polished with BAS polishing kit (Bioanalytical Systems, Inc., USA) and alumina powder (0.05 μm) to mirror finish and ultrasonicated in double distilled water for 3 min. Prior to the electrochemical experiments, the buffer solution was deoxygenated with nitrogen for 10 min. UV–visible spectra were obtained using Hitachi U-3300 spectrophotometer (Japan).

2.3. Preparation of PBCB and PBCB-MWCNT electrodes

The PBCB modified electrode was prepared by the electropolymerization of BCB monomers in neutral solution using bare GCE electrode. The electro-active system was electro-generated in situ from BCB oxidation, the electrode applied in the potential range of -0.6–1.0 V (vs. Ag/AgCl) with scan rate of 100 mV s^{-1} and different scan cycles (or segments) in 0.1 M PBS (pH 7) containing 1×10^{-4} M BCB monomers. We focused on the scan segments of BCB electropolymerization to be an important parameter for controlling PBCB film formation. So there are several scan segments including 40, 120, 240, and 720 segments result in different PBCB films with representation of PBCB-40seg, PBCB-120seg, PBCB-240seg, and PBCB-720seg, respectively.

The PBCB-MWCNT modified electrode was prepared by the electropolymerization of BCB monomers in neutral solution using MWCNT-modified GCE (MWCNT/GCE). Prior to the electropolymerization of BCB the GCE was firstly coated with MWCNT which was functionalized with carboxylic group by acidic treatment. The electro-active system was electro-generated in situ from BCB oxidation, the MWCNT/GCE electrode applied as the same PBCB formation process as previous mentioned.

The modified electrodes including PBCB/GCE, PBCB/ITO, PBCB-MWCNT/GCE and PBCB-MWCNT/ITO, with different scan segments were stored in the refrigerator at 4 ℃ for further study in this work.

3. RESULTS AND DISCUSSION

3.1. Different PBCB film formation on GCE and MWCNT/GCE

Approach a low cost counter electrode using active PBCB film is controlled by the scan segments of BCB electropolymerization on bare GCE or MWCNT/GCE. Therefore, the PBCB film formation involving the electropolymerization of BCB monomers was investigated by cyclic voltammetry using GCE and MWCNT/GCE, respectively.
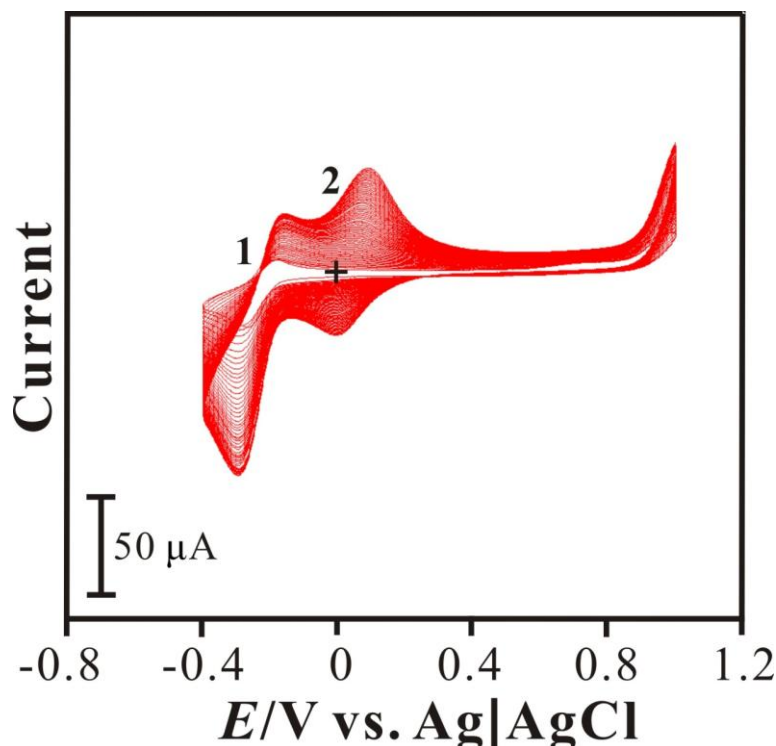

Figure 1. Cyclic voltammograms of PBCB film formation at MWCNT/GCE in pH 7 PBS containing 1×10^{-4} M BCB. Scan rate = 0.1 Vs^{-1}. Scan segments = 120.

Fig. 1 displays the consecutive cyclic voltammograms of BCB electropolymerzation in pH 7 PBS using MWCNT/GCE. There are two well-defined redox couples with formal potential of $E^{0'}_1 = -221$ mV, $E^{0'}_2 = 13$ mV (vs. Ag/AgCl) observed for MWCNT/GCE. The redox couple 1 & 2 is attributed to the reduced and oxidized forms of BCB monomer and PBCB polymer [40 − 42], respectively. The redox peak current develops more higher as increasing the scan segments for using MWCNT when compared with the case using bare GCE. This might indicate that the MWCNT enhance the cathodic peak current for BCB monomer. It is similar to our previous result [43] and it means that the MWCNT provides more surface areas to load more PBCB. It also provides a hint to load more active PBCB species by controlling scan segments in the prepared process of PBCB film formation. Therefore, the different scan segments are designed for different PBCB amounts deposited on electrode surface especially on the MWCNT-modified electrode surface for further study.

3.2. UV-Visible spectra characteristics of PBCB-MWCNT composites

The active species of BCB, MWCNT, PBCB, and hybrid matrix are characterized by UV-Visible spectroscopy.

Fig. 2A shows the UV-Visible spectra of these active species dissolved in 0.1 M PBS (pH 7). It's obviously to see that the obvious absorption peaks at 579 nm and 631 nm represented for BCB monomer similar to previous results [44,45]. By examining the structure of BCB, it is noted that BCB provides electrostatic interaction, π-π interaction, dipole-dipole interaction, and hydrogen bonding [44]. No chemical reaction due to no new absorption peak appears in the mixing BCB and MWCNT solution. It also means that the BCB can stay stably with MWCNT in the hybrid composite.
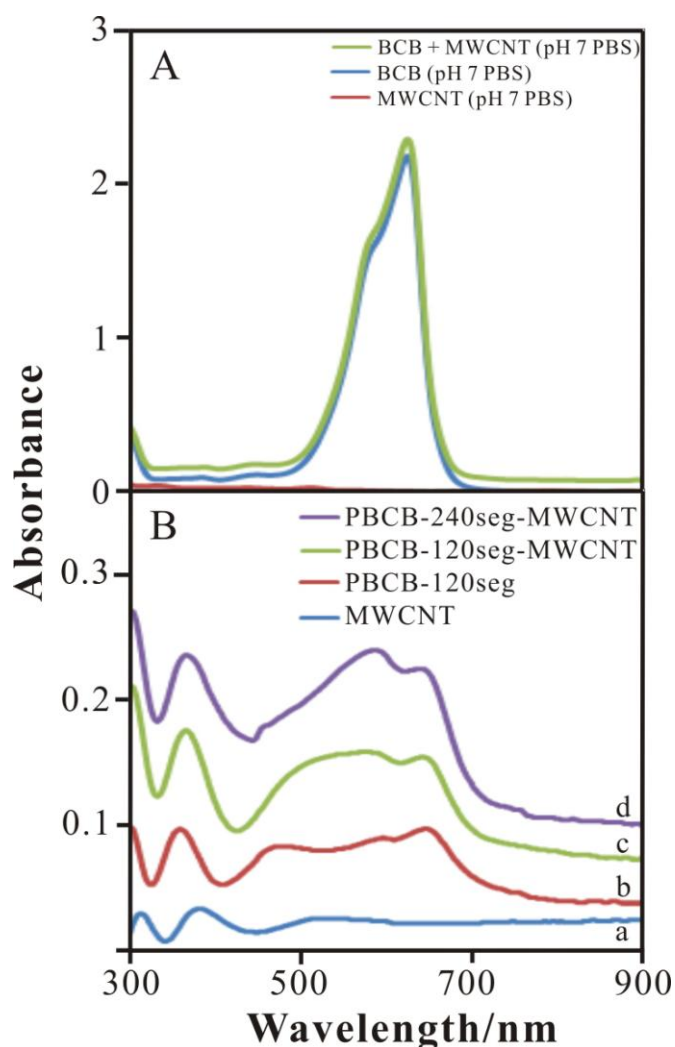

Figure 2. Absorption spectra of active species: (A) dissolved in PBS solution and (B) formed on ITO electrode surface. (a) MWCNT, (b) PBCB-120seg, (c) PBCB-120seg-MWCNT, and (d) PBCB-240seg-MWCNT modified ITO electrodes were prepared in 0.1 M PBS (pH 7).

Fig. 2B shows the UV-Visible spectra of active PBCB species formed on bare ITO and MWCNT/ITO prepared in 0.1 M PBS (pH 7) with different scan segments. The absorption peaks are measured and shown in Table 1. It's obviously to see that the hybrid composites almost maintain the

spectroscopic properties of original single components except of slightly red shift in the absorption peaks. This might be due to the slight pH effect caused by the difference between the species dissolved in PBS solution and coated on ITO. Furthermore, more PBCB amount controlled by scan segments is proved due to the much higher absorption intensity.

The observation of well-defined and the persistent absorption peaks indicate that these active species exhibit spectra characteristics on the electrode surface.

Table 1. Absorption peaks of active species examined by UV-Visible spectroscopy.

Sample Type	Active species	Absorption peak/nm
Solution (pH 7 PBS)	MWCNT	No obvious peaks
	BCB	579, 631
	BCB + MWCNT	579, 631
Film modified on ITO	MWCNT/ITO	321, 392
	PBCB-120seg[a]	371, 607, 656
	PBCB-120seg[a]-MWCNT	372, 602, 654
	PBCB-240seg[a]-MWCNT	377, 599, 651

[a] seg: the scan segment for preparation of PBCB.

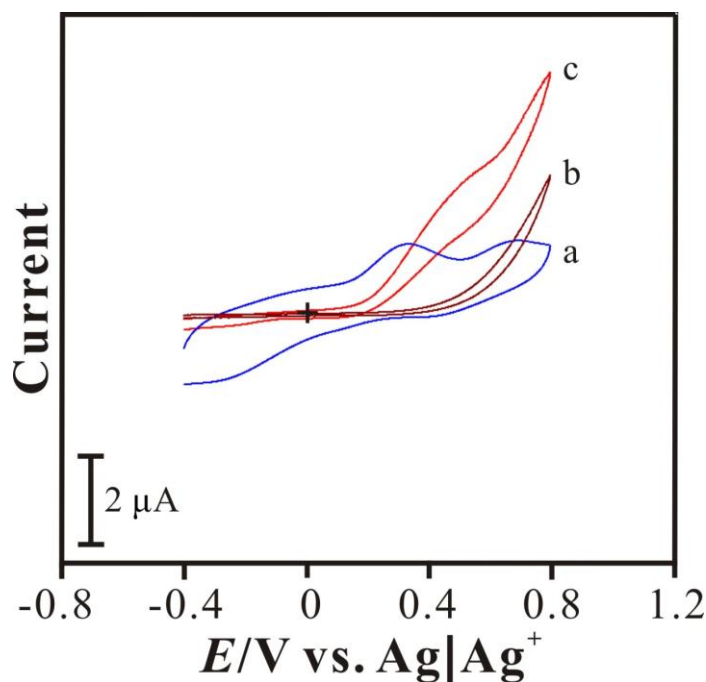### 3.3. Electrocatalytic properties of PBCB and PBCB-MWCNT films

Figure 3. Cyclic voltammograms of (a) PBCB-720seg-MWCNT, (b) PBCB-120seg, and (c) PBCB-120seg-MWCNT, obtained in acetonitrile solution containing 0.1 M LiClO$_4$, 10 mM LiI, and 1 mM I$_2$. Scan rate = 100 mVs^{-1}.

The electroactive species, PBCB and PBCB-MWCNT, were investigated for the electrocatalytic reaction of I_2/I_3^- and I_3^-/I^- transfer processes.

Fig. 3 shows the voltammograms of different modified electrodes including (a) PBCB-720seg-MWCNT/GCE, (b) PBCB-120seg/GCE, and (c) PBCB-120seg-MWCNT/GCE prepared in pH 7 PBS. Compared to the PBCB modified electrode without MWCNT (as shown in curve b), the much obvious redox couples of I_2/I_3^- and I_3^-/I^- transfer processes are found at both PBCB and MWCNT-modified electrodes as shown in curve a & b. This means that the rich surface areas contributed by MWCNT to lower charge-transfer resistance and higher electrocatalytic activity. Particularly, the hybrid composite prepared with higher scan segments shows the more closed peak-to-peak separation and more reversible processes. It indicates that the electron transfer is becoming fast at higher PBCB deposition amount on MWCNT/GCE. This is one of the methods approaching to a low cost counter electrode for dye-sensitized solar cells.

3.4. DSSCs photovoltaic properties using PBCB and PBCB-MWCNT films

DSSCs photovoltaic properties were investigated by PBCB and PBCB-MWCNT films with different PBCB deposition amount prepared by scan segments including 40, 120, and 240 segments, respectively.

Fig. 4 illustrates the photocurrent-voltage curves of the cells with PBCB–120seg, PBCB–40seg-MWCNT, PBCB–120seg-MWCNT, PBCB–240seg-MWCNT, and Pt counter electrodes, respectively. The open-circuit voltage (V_{oc}), short-circuit photocurrent density (J_{sc}), fill factor (FF) and efficiency (η) of the cells are listed in Table 2. Energy conversion efficiency of the DSSCs using the PBCB–MWCNT composite film with different PBCB amount can be used as a counter electrode with the performance values of J_{sc} and V_{oc} approaching to those of the DSSCs with Pt counter electrode. However, the difference of fill factors between PBCB–MWCNT and Pt limited the performance.

Compared to PBCB film (PBCB-120seg), the addition of a small amount of MWCNT (PBCB-120seg-MWCNT) effectively affected the efficiency of the cells with about 10 times. This is mainly due to that the high specific surface area providing high catalytic activity toward reduction of iodine [46]. To investigate the effects of PBCB content on the performances of DSSCs, a series of counter electrodes were prepared by different PBCB content in the PBCB-MWCNT hybrid composite by controlling scan segment in the PBCB preparation. As the PBCB deposition in the mixture increased from 120 to 240 scan segments, the energy conversion efficiency of the DSSC was increased from 0.23% to 0.33% (as shown in Table 2). However, further increasing the scan segment in the PBCB preparation procedure showed little affect on the energy conversion efficiency of the cells. These results indicate that a deposition limit of PBCB. In our result, a limit of scan segments (related to PBCB deposition amount) is 300 segments and 450 segments for using a bare electrode and a MWCNT-modified electrode, respectively. Although the efficiency is low currently, it is still valuable to understand the important information for this hybrid composite modified counter electrode. First, the MWCNT is necessary to use due to its large active surface area. Second, the MWCNT modified electrode can load more PBCB deposition amount on the counter electrode. Third, the efficiency is

increasing while the active species deposition is increasing. It is approaching to a low cost counter electrode by increasing PBCB deposition on MWCNT modified electrode.
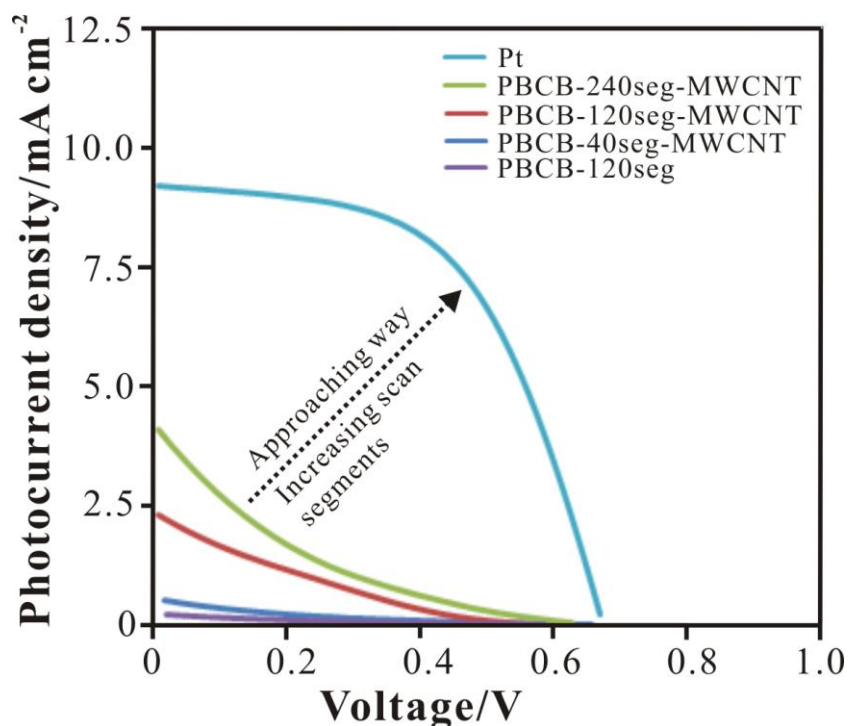

Figure 4. $J-V$ characteristics of DSSCs employing Pt and PBCB (prepared under 0.1 M PBS containing 1×10^{-4} M BCB monomer controlled by different scan segments: 40, 120, 240 segments with/without MWCNT) counter electrodes measured under AM 1.5, 100 mW cm^{-2} front-and rear-illumination. The active area is 0.25 cm^2.

By above results, one can conclude that the PBCB-MWCNT is a good electroactive species as catalyst to be one of the material options with lower electron transfer resistance and higher current response. And the scan segments of PBCB preparation which is able to adjust the PBCB deposition amount and it is the important control parameter to approaching to a low cost counter electrode. Therefore, we propose this is the method to approaching a low cost counter electrode for dye-sensitized solar cells.

Table 2. Cell performance of the DSSCs with different counter electrodes.

Counter electrodes	J_{sc}/mA cm^{-2}	V_{oc}/V	*FF*/%	η/%
PBCB-120seg[a]	0.19	0.56	16.44	0.02
PBCB-120seg[a]-MWCNT	2.44	0.60	13.52	0.23
PBCB-240seg[a]-MWCNT	3.30	0.62	12.25	0.33
Pt	16.27	0.71	48.54	5.61

[a] seg: the scan segment for preparation of PBCB.

4. CONCLUSIONS

In summary, the PBCB and PBCB–MWCNT composites can be prepared by BCB electropolymerization on bare electrode and MWCNT-modified electrode. They are active for I_2/I_3^- and I_3^-/I^- redox processes especially for PBCB-MWCNT composite. The MWCNT provides more active surface area for the reaction and more space to load PBCB deposition amount. The observation of well-defined and the persistent absorption peaks indicate that the PBCB-MWCNT active species exhibit more PBCB deposition amount by the higher intensity of spectra characteristics for the PBCB-MWCNT electrode through more scan segments in the PBCB preparation procedure. Particularly, the PBCB deposition amount can be increased by increasing the scan segments in the PBCB preparation procedure result in the increase of cell efficiency. Although the efficiency is low currently, it is still valuable to understand the important information for this hybrid composite modified counter electrode. First, the MWCNT is necessary to use due to its large active surface area. Second, the MWCNT modified electrode can load more PBCB deposition amount on the counter electrode. Third, the efficiency is increasing while the active species deposition is increasing. It is approaching to a low cost counter electrode by increasing PBCB deposition on MWCNT modified electrode.

References

1. M. Grätzel, *J. Photochem. Photobiol. C* 4 (2003) 145.
2. M. Grätzel, *Inorg. Chem.* 44 (2005) 6841.
3. B. O'Regan, M. Grätzel, *Nature* 353 (1991) 373.
4. R. Jose, V. Thavasi, S. Ramakrishna, *J. Am. Ceram. Soc.* 92 (2009) 289.
5. Mishra, M.K.R. Fischer, P. Bäuerle, *Angew. Chem., Int. Ed.* 48 (2009) 2474.
6. M. Gorlov, L. Kloo, *Dalton Trans.* (2008) 2665.
7. T.N. Murakami, M. Grätzel, *Inorg. Chim. Acta* 361 (2008) 572.
8. A. Kay, M. Gratzel, *Sol. Energy Mater. Sol. Cells* 44 (1996) 99.
9. K. Suzuki, M. Yamaguchi, M. Kumagai, S. Yanagida, *Chem. Lett.* 23 (2003) 28.
10. G. Wang, W. Xing, S. Zhuo, *J. Power Sources* 194 (2009) 568.
11. S.I. Cha, B.K. Koo, S.H. Seo, Dong Y. Lee, *J. Mater. Chem.* 20 (2010) 659.
12. P. Joshi, Y. Xie, M. Ropp, D. Galipeau, S. Bailey, Q. Qiao, *Energy Environ. Sci.* 2 (2009) 426.
13. S.C. Feng, L. Jing, L.T. Zhan, C. Jun, S.X. Rui, *J. Power Sources* 177 (2008) 631.
14. J.B. Xia, N. Masaki, K.J. Jiang, S. Yanagida, *J. Mater. Chem.* 17 (2007) 2845.
15. S. Ahmad, J.H. Yum, X.X. Zhang, M. Gratzel, H.J. Butt, *J. Mater. Chem.* 20 (2010) 1654.
16. Z. Li, B. Ye, X. Hu, X. Ma, X. Zhang, Y. Deng, *Electrochem. Commun.* 11 (2009) 1768.
17. H. Sun, Y. Luo, Y. Zhang, D. Li, Z. Yu, K. Li, Q. Meng, *J. Phys. Chem. C* 114 (2010) 11673.
18. J. Xia, L. Chen, S. Yanagida, *J. Mater. Chem.* 21 (2011) 4644.
19. S.S. Jeon, C. Kim, J. Ko, S.S. Im, *J. Mater. Chem.* 21 (2011) 8146.
20. K.M. Lee, C.Y. Hsu, P.Y. Chen, M. Ikegami, T. Miyasaka, K.C. Ho, *Phys. Chem. Chem. Phys.* 18 (2009) 3375.
21. T.N. Murakami, S. Ito, Q. Wang, M.K. Nazeeruddin, T. Bessho, I. Cesar, P. Liska, R. Humphry-Baker, P. Comte, P. Péchy, M. Grätzel, *J. Electrochem. Soc.* 153 (2006) a2255.

22. Y. Saito, W. Kubo, T. Kitamura, Y. Wada, S. Yanagida, *J. Photochem. Photobiol. A* 164 (2004) 153–157.
23. T.C. Wei, Y.Y. Wang, C.C. Wan, *Appl. Phys. Lett.* 88 (2006) 103122.
24. T.C. Wei, C.C. Wan, Y.Y. Wang, C.M. Chen, H.S. Shiu, *J. Phys. Chem. C* 111 (2007) 4847.
25. A.P. Periasamy, Y.H. Ho, S.M. Chen, *Biosens. Bioelectron.* 29 (2011) 151.
26. K.C. Lin, T.H. Tsai, S.M. Chen, *Biosens. Bioelectron.* 26 (2010) 608.
27. S. Thiagarajan, T.H. Tsai, S.M. Chen, *Biosens. Bioelectron.* 24 (2009) 2712.
28. Y. Li, J.Y. Yang, S.M. Chen, *Int. J. Electrochem. Sci.* 6 (2011) 4829.
29. Y. Umasankar, S.H. Wang, S.M. Chen, *Analytical Methods* 3(11) (2011) 2604.
30. S. Shahrokhian, E. Asadian, *Electrochim. Acta*, 55 (2010) 666.
31. N. Li, M. Zhu, M. Qu, X. Gao, X. Li, W. Zhang, J. Zhang, J. Ye, *J. Electroanal. Chem.* 651 (2011) 12.
32. K.C. Lin, Y.C. Lin, S. M. Chen, *Analyst* 137 (2012) 1378.
33. B. Unnikrishnan, Y. Umasankar, S.M. Chen, C.C. Ti, *Int. J. Electrochem. Sci.* 7 (2012) 3047.
34. Y. Umasankar, B. Unnikrishnan, S.M. Chen, T.W. Ting, *Int. J. Electrochem. Sci.* 7 (2012) 484.
35. Y. Umasankar, T.Y. Huang, S.M. Chen, *Anal. Biochem.* 408 (2011) 297.
36. Y. Li, S. Y. Yang , S. M. Chen, *Int. J. Electrochem. Sci.* 6 (2011) 3982.
37. J.Y. Yang, Y. Li, S.M. Chen, K.C. Lin, *Int. J. Electrochem. Sci.* 6 (2011)2235.
38. M.E. Ghica, C.M.A. Brett, *J. Electroanal. Chem.* 629 (2009) 35.
39. Y. Umasankar, T.W. Ting, S.M. Chen, *J. Electrochem. Soc.* 158 (2011) K117.
40. M. Chen, J.Q. Xu, S.N. Ding, D. Shan, H.G. Xue, S. Cosnier, M. Holzinger, *Sens. Actuators B* 152 (2011) 14.
41. Y. Umasankar, T.W. Ting, S.M. Chen, *J. Electrochem. Soc.* 158 (2011) K117.
42. M. Chen, J.Q. Xu, S.N. Ding, D. Shan, H.G. Xue, S. Cosnier, M. Holzinger, *Sens. Actuators B* 152 (2011) 14.
43. K.C. Lin, J.Y. Huang, S.M. Chen, *Int. J. Electrochem. Sci.* 7 (2012) 9161.
44. Y. Zhang, T. H. Pham, M. S. Pena, R.A. Agbaria, I. M. Warner, *Appl. Spectrosc.* 52 (1998) 952.
45. S.A. Kumar, S.F. Wang, Y.T. Chang, *Thin Solid Films* 518 (2010) 5832.
46. J.E. Trancik, S.C. Barton, J. Hone, *Nano Lett.* 8 (2008) 982.